Original Article

Institution of MECHANICAL ENGINEERS
Journal of SYSTEMS AND CONTROL ENGINEERING

Proc IMechE Part I:
J Systems and Control Engineering
2021, Vol. 235(6) 984–991

DOI: 10.1177/0959651820953275
journals.sagepub.com/home/pii
SAGE

Path tracking control of electromechanical micro-positioner by considering control effort of the system

Mohammad Reza Gharib, Ali Koochi and Mojtaba Ghorbani

Abstract

Position controlling with less overshoot and control effort is a fundamental issue in the design and application of micro-actuators such as micro-positioner. Also, tracking a considered path is very crucial for some particular applications of micro-actuators such as surgeon robots. Herein, a proportional–integral–derivative controller is designed using a feedback linearization technique for path tracking control of a cantilever electromechanical micro-positioner. The micro-positioner is simulated based on a 1-degree-of-freedom lumped-parameter model. Three different paths are considered, and the capability of the designed controller on the path tracking with lower error and control effort is investigated. The obtained results demonstrate the efficiency of the designed proportional–integral–derivative controller not only for reducing the tracking error but also for decreasing the control effort.

Keywords

Feedback linearization, micro-electromechanical system, micro-positioner, path tracking, proportional–integral–derivative controller

Date received: 24 March 2020; accepted: 30 July 2020

Introduction

These days, many scientists, as well as researchers, have devoted themselves to the quest of micro/nano-electromechanical system (MEMS/NEMS) technologies because of its astonishing potential in the field of fundamental research, as well as application in industrial engineering. Micro-positioner is an MEMS device that can utilize for positioning, orienting, and applying a force in various branches of science and engineering.[1] Micro-positioners have been used widely in the different miniature structures, including but not limited to scanning tunneling microscopy, atomic force microscopy, and ultrahigh-density probe storage systems.[2–4] There are several actuation techniques in the micro-positioners, such as electrostatic, electromagnetic, electro-thermal, and piezoelectric. Among these methods, electrostatic actuation is the most popular mechanism due to its simplicity, small actuation voltage, and as it requires limited mechanical components.[5] Electrostatic actuation usually relies on parallel plate capacitors. This actuation technique does not manufacture from special material such as piezoelectric or exited by external fields like electromagnetic. The sole requirement is the voltage difference, which is available in all electronic circuits. It is worth to note that the operating range of the micro-positioner is limited by the pull-in phenomenon. By applying a voltage difference between moveable and fixed electrodes, the electrical force moves the moveable part toward the fixed plane. At a critical voltage known as "pull-in voltage," the electrical force overcomes the mechanical restoring force, which results in additional deflection of the moveable electrode. This leads to an increase in electrical potential in a positive feedback loop. Previous researchers have studied the pull-in instability threshold and investigate the impact of the various physical phenomena on

Department of Mechanical Engineering, University of Torbat Heydarieh, Torbat Heydarieh, Iran

Corresponding author:
Mohammad Reza Gharib, Department of Mechanical Engineering, University of Torbat Heydarieh, Torbat Heydarieh, Razavi Khorsan Province 9516168595, Iran.
Email: m.gharib@torbath.ac.ir

the pull-in voltage and pull-in deflection of nano-actuators.[5–9]

Control techniques might be employed to avoid the undesired outcomes of pull-in instability and improve the performance of a micro-positioner. An electrostatic MEMS can be controlled by a voltage[10–13] or charge source.[14] The voltage control not only has a well-known dynamic but also its complexity is less than charge control. Various linear and nonlinear control approaches have been presented by the previous researcher for MEMS.[15] Tzes et al.[15] used a 1-degree-of-freedom (1-DOF) model to simulate the behavior of a capacitor micro-actuator. They neglect the fringing field effect and design a multi-parameter H_∞ controller to control the displacement of micro-actuator. Vagia et al.,[16] from 2006 to 2013, developed numerous controllers for controlling the deflection of electromechanical micro-actuators, including, intelligent robust controller, robust proportional–integral–derivative (PID),[17] and robust adaptive.[18] A linear parameter-varying methodology is employed for controlling an electrostatic micro-actuator in Shirazi et al.[12] Recently, some researchers focus on the suppression of vibration and position control of the MEMS to increase their performances. Some of the most remarkable research works in the mentioned fields are sliding mode control,[19,20] fuzzy control,[21,22] robust control,[23] PID[17] controller, and so on. However, all of these researchers focus on the position control of the MEMS, and the path tracking control of MEMS has not been comprehensively addressed. While for some applications such as positioning, switching, and force applying, the position control is dominant, for some special application such as biological purposes, the path tracking control should be considered.

In the present work, the feedback linearization technique is incorporated with the PID method to design a vibration suppression controller for an electromechanical micro-positioner. The micro-positioner is modeled as an Euler–Bernoulli cantilever beam. A 1-DOF lumped-parameter model is employed for simplifying the voltage deflection relation of micro-positioner. The proposed controller is not only suitable for stabilizing the electromechanical micro-positioner vibrations but also is capable of path tracking control.

In the rest of this article, the fundamentals of the proposed model and derivation of the governing equations of micro-positioner are presented in section "Modeling." In section "Micro-positioner controller design," the nonlinear controller is developed based on the feedback linearization. In section "Results and discussion," the controller is applied to micro-positioner, its ability for tracking three different paths are investigated, and both tracking error and control effort are discussed. Finally, in section "Conclusion," the conclusions are drawn.

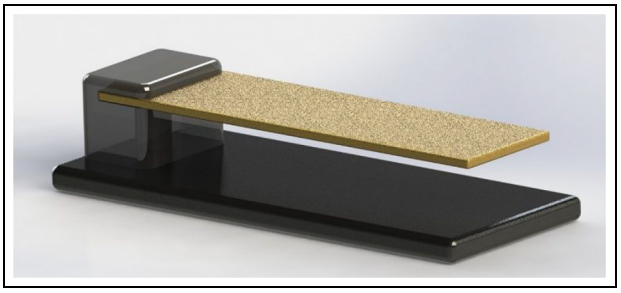

Figure 1. The schematic representation of a typical micro-positioner.

Modeling

Figure 1 shows the schematic view of a typical micro-positioner constructed from a moveable electrode suspended over a fixed plate. The movable part of the positioner is a cantilever beam with the length of L, the width of b, and the thickness of h. The initial gap between the movable arm and fixed ground is g. Applying the voltage difference between the moveable and fixed electrodes results in an electrical field, which leads to the bending of the movable electrode. This deflection of beam tip can be used for positioning, transmitting objects in arbitrary paths, or applying force to another system.

The nonlinear governing equations of cantilever micro-positioner can be explained as

$$\rho A \frac{\partial^2 w}{\partial t^2} + EI \frac{\partial^4 w}{\partial x^4} = F_E + F_D \tag{1}$$

where ρ is the mass density, A is the micro-positioner cross-sectional area, E is the Young modulus, I is the cross-sectional moment of inertia, F_E is the electrical force, and F_D is the damping force.

Considering the electrical field of a parallel plate capacitor, the governing equation can be obtained as

$$F_E = \frac{\varepsilon b L V^2}{2g^2} \tag{2}$$

where ε is the dielectric constant. By applying a voltage difference between the moveable electrode and ground, the electrical field results in beam deflection. Therefore, the initial gap between the moveable part and a fixed plate reduced for g to $g - w$. Accordingly, the electrical force acts to a deflected actuator is modified as

$$F_E = \frac{\varepsilon b L V^2}{2(g - w)^2} \tag{3}$$

The damping force is related to the damping coefficient (C) and the speed

$$F_D = -C \frac{\partial w}{\partial t} \tag{4}$$

It is worth to note that the resource for damping in NEMS/MEMS includes thermoplastic damping, surface phonon scattering, and viscous damping (squeezed film damping, slide film damping, and drag force).

Using a single DOF lumped-parameter model is a useful method to simplify MEMS/NEMS analysis.[24,25] To this end, the micro-actuator shown in Figure 1 is approximated by a rigid plate suspended by spring over a fixed ground, as shown in Figure 2. In this method, the micro-positioner deflection is assumed to be constant along the length. In the lumped-parameter model, defining the efficient mass and the efficient spring constant is very crucial. These parameters can be investigated using the experiential approaches, the numerical solution, or the analytical method. For a cantilever Euler–Bernoulli beam, the effective spring constant in the lumped-parameter model is given as[26]

$$K = \frac{8EI}{L^3} \tag{5}$$

Finally, the 1-DOF model of micro-positioner is given by

$$m\ddot{w} + C\dot{w} + Kw = \frac{\varepsilon b L V^2}{2(g-w)^2} \tag{6}$$

The micro-positioner operating range depends on the applied direct current (DC) voltage. At equilibrium point w_i, the positioner speed and acceleration are zero (i.e.$\dot{w}_i = \ddot{w}_i = 0$); hence, equation (1) yields

$$Kw_i = \frac{\varepsilon b L {V_0}^2}{2(g-w_i)^2} \tag{7a}$$

$$V_0 = \left[\frac{2Kw_i(g-w_i)^2}{\varepsilon b L}\right]^{\frac{1}{2}} \tag{7b}$$

This means for manipulating the micro-positioner to the distance w_i from its free-standing position, the nominal voltage V_0 should be applied to the system.

Micro-positioner controller design

The controller design aims to track the desired path and to stabilize vibrations of the system caused by the initial velocity or displacement of the micro-beam.

Restriction of the path planning

To prevent mechanical damage and create significant tensions, it is necessary to make the input applied to the sensor carefully designed. The constraints considered for eligible inputs are listed as follows:

- The stable range of the beam motion should be considered. This stable range is limited by the pull-in phenomena. The pull-in voltage can be obtained by setting $\partial V_0/\partial w_i = 0$. Using equation (7b), the pull-in deflection is obtained as $w_{PI} = g/3$. Therefore, the stable actuation ranges of micro-positioner due to its inherent instability are $0 \leqslant w \leqslant g/3$.
- The motion of the beam during the desired path should have a minimum jerk or higher degrees of acceleration. The jerk can undesirably affect the controller efficiency and stabilization of the system. Moreover, by minimizing the jerk, the vibrations of micro-positioners are reduced.

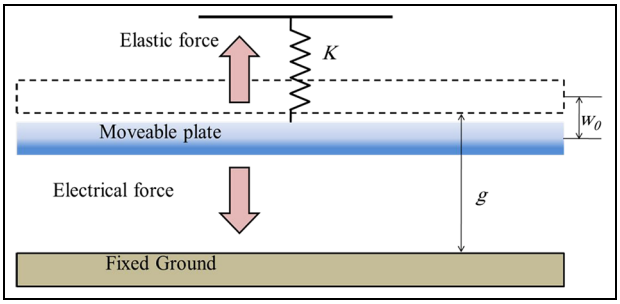

Figure 2. 1-DOF lumped-parameter model.

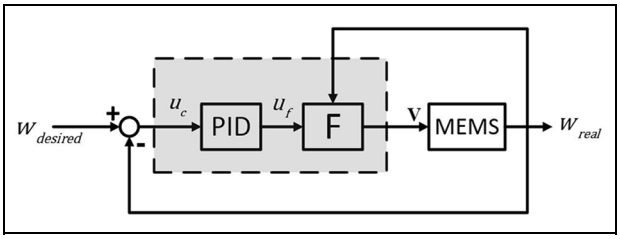

Figure 3. The system control block diagram.

Feedback linearization

Feedback linearization is an efficient method of nonlinear control design, which has engaged a great deal of research interest in recent years. The main idea of the mentioned technique is to transform the dynamics of a nonlinear system into a (partly or wholly) linear one. In the next step, a linear control approach can be applied to the system. The ultimate goal of feedback linearization in this article is to figure out a relationship between the outputs and the control inputs. This is obtained by determining a feedback law and a change of coordinates that transform a nonlinear system into a linear and controllable one. The control block diagram of the system is illustrated in Figure 3.

First, for the linearization of the system using the nonlinear motion equation of the system, the following relation is presented

$$V = (g-w)\sqrt{\frac{2}{\varepsilon b L}u_f} \tag{8}$$

By combining equations (6) and (8), the following linear equation is obtained

$$m\ddot{w} + C\dot{w} + Kw = \frac{\varepsilon bL}{2(g-w)^2}\left[(g-w)\sqrt{\frac{2}{\varepsilon bL}u_f}\right]^2 \quad (9)$$

The system state space can also be displayed as follows

$$\begin{cases} \overbrace{\begin{bmatrix}\dot{w}\\ \ddot{w}\end{bmatrix}}^{\dot{X}} = \overbrace{\begin{bmatrix}0 & 1\\ -\frac{K}{m} & -\frac{K}{m}\end{bmatrix}}^{A_{sys}}\overbrace{\begin{bmatrix}w\\ \dot{w}\end{bmatrix}}^{X} + \overbrace{\begin{bmatrix}0\\ \frac{1}{m}\end{bmatrix}}^{B_{sys}}u_f \\ \underbrace{w}_{Y} = \underbrace{\begin{bmatrix}1 & 0\end{bmatrix}}_{C_{sys}}\begin{bmatrix}w\\ \dot{w}\end{bmatrix} + \underbrace{0}_{D_{sys}}u_f \end{cases} \quad (10)$$

where

$$u_f = \frac{\varepsilon bL}{2(g-w)^2}\left[(g-w)\sqrt{\frac{2}{\varepsilon bL}u_f}\right]^2 \quad (11)$$

Concerning the above equation, the transfer function from u_f to Y is determined. With the help of the Laplace transform, from equation (10), one obtains

$$\frac{Y(s)}{u_f(s)} = \frac{1}{ms^2 + Cs + K} \quad (12)$$

Since m, K, and C are positive, the system does not have any polarities on the right of the coordinate axis. So, the system is always stable for $0 \leqslant w \leqslant g/3$.

Now, for this stable linear system, a PID controller is designed as follows

$$\mathrm{PID}(s) = 7.1701 + \frac{72,285.3716}{s} + 0.0001\frac{507,148.5812}{1 + \frac{507,148.5812}{s}} \quad (13)$$

Uncertainty in the feedback path

In equation (8), the control signal is introduced, and the stability of the system is investigated, but this method relies on the accurate detection of the actuator. One of the most important problems with electronic and mechanical systems is their uncertainties. There are different types of uncertainties in these systems. For example, incorrect position detection, inherent geometric, disturbances, noise signals, inertial, calculation error, and some nonlinearities could not be easily circumvented in practice.

Therefore, given the above explanation, it is necessary to assume equation (8) as follows

$$V = (g - \tilde{w})\sqrt{\frac{2}{\varepsilon bL}u_f} \quad \tilde{w} \to w, \tilde{w} \neq w \quad (14)$$

By combining equations (6) and (13), the following results will be obtained

$$m\ddot{w} + C\dot{w} + Kw = \frac{\varepsilon A}{2(g-w)^2}\left[(g-\tilde{w})\sqrt{\frac{2}{\varepsilon A}u_f}\right]^2 \quad (15)$$

The state-space model of the system is shown below

$$\begin{cases} \overbrace{\begin{bmatrix}\dot{w}\\ \ddot{w}\end{bmatrix}}^{\dot{X}} = \overbrace{\begin{bmatrix}0 & 1\\ -\frac{K}{m} & -\frac{C}{m}\end{bmatrix}}^{A_{sys}}\overbrace{\begin{bmatrix}w\\ \dot{w}\end{bmatrix}}^{X} + \overbrace{\begin{bmatrix}0\\ 1+\bar{\alpha}\end{bmatrix}}^{B_{sys}}m^{-1}u_f \\ \underbrace{w}_{Y} = \underbrace{\begin{bmatrix}1 & 0\end{bmatrix}}_{C_{sys}}\begin{bmatrix}w\\ \dot{w}\end{bmatrix} + \underbrace{0}_{D_{sys}}u_f \end{cases} \quad (16)$$

Since the values of K, C, and m are positive, then the matrix $\mathbf{A_{sys}}$ has no eigenvalue on the right-hand axis, which is called the Hurwitz matrix.

According to Lyapunov's theorems, for any given positive $\mathbf{Q}$ matrix, there exists a positive matrix $\mathbf{P}$ that applies to the following relation

$$\mathbf{A}_{sys}^T + \mathbf{A}_{sys}\mathbf{P} = -\mathbf{Q} \quad (17)$$

If the Lyapunov function is assumed as follows, we have

$$\mathbf{V} = \mathbf{X}^T\mathbf{P}\mathbf{X} + \boldsymbol{\nu}^T\boldsymbol{\Gamma}\boldsymbol{\nu} \quad (18)$$

where $\boldsymbol{\Gamma}$ is the positive matrix. The derivation of the above equation results in

$$\dot{\mathbf{V}} = \dot{\mathbf{X}}^T\mathbf{P}\mathbf{X} + \mathbf{X}^T\mathbf{P}\dot{\mathbf{X}} + \dot{\boldsymbol{\nu}}^T\boldsymbol{\Gamma}\boldsymbol{\nu} + \boldsymbol{\nu}^T\boldsymbol{\Gamma}\dot{\boldsymbol{\nu}} \quad (19)$$

According to the above equation, $\boldsymbol{\Gamma}$ is the definite positive matrix, so $\dot{\boldsymbol{\nu}}^T\boldsymbol{\Gamma}\boldsymbol{\nu} = \boldsymbol{\nu}^T\boldsymbol{\Gamma}\dot{\boldsymbol{\nu}}$. Consequently, using equation (16), we have

$$\dot{\mathbf{V}} = -\mathbf{X}^T\mathbf{Q}\mathbf{X} + 2\boldsymbol{\nu}^T\left(\mathbf{m}^{-T}\mathbf{B}^T\mathbf{P}\mathbf{X} + \boldsymbol{\Gamma}\dot{\boldsymbol{\nu}}\right) \quad (20)$$

Given equation (20), suppose the following equation

$$\dot{\boldsymbol{\nu}} = -\boldsymbol{\Gamma}^{-1}\mathbf{m}^{-T}\mathbf{B}^T\mathbf{P}\mathbf{X} \quad (21)$$

The derivative of the Lyapunov function will always be negative

$$\dot{\mathbf{V}} = -\dot{\mathbf{X}}^T\mathbf{Q}\mathbf{X} \quad (22)$$

As a result, based on Lyapunov's second theorem, the system will always be stable. Therefore, it can be claimed that the controller introduced in this article is always capable of controlling the system and will not be unstable.

Results and discussion

In the previous part, the linear system is achieved. In this section, the designed controller is tested on a typical micro-positioner to prove the control strategy. The geometrical and mechanical properties of the micro-positioner are presented in Table 1. A system with

Table 1. The geometrical and mechanical properties of the micro-positioner.[17]

Parameter	Description	Value
M	Mass	7.0496×10^{-10} kg
K	Stiffness of the spring	0.816 N/m
C	Damping coefficient	1.4×10^{-5} kg
B	Moveable arm width	400 μm
L	Moveable arm length	400 μm
G	Initial gap	4 μm

similar geometrical and material properties is investigated by Vagia et al.[17] They design a PID controller for controlling the position of a micro-actuator. In this article, we try to design a new controlling system for path tracking of a micro-actuator. A block diagram of the controlling system is shown in Figure 3. The goal of the controller is to move the micro-positioner from the initial position to the desired one by satisfying the following condition:

1. The system should track the considered path.
2. The system should have a minimum of overshoot.
3. The control effort should be lower.

To test the path tracking of the designed controller, three arbitrary paths are considered.

Efficient controller selection

To choose a controller, consider the features and applications of the system to understand what type of controller fits for the system is needed. In general, there are no better controllers, so researchers are always looking for the most suitable compensators and filters to control systems. The term "most appropriate" is sometimes used to mean high precision for tracking, and sometimes to define the minimum energy to control the system (control effort). Therefore, a controller should be selected according to the conditions of the system.

The authors, by carefully studying the work of other researchers, found weaknesses in the performance of the methods presented by others. For example, researchers have considered the input path to the system arbitrary, while the nature of the system does not allow for the use of any path such as jerk in path tracking. So, it is necessary to design the path tracking, which does not damage the system (MEMS). In this article, in addition to the stability margins of closed-loop systems and track input paths accurately, the control effort of the system for tracking paths is considered.

Path tracking

The ultimate aim of a path-tracking controller of a micro-positioner is to minimize the distance between the actuator (micro-positioner) motion and the defined path (or reference point) and limit the control effort of the system to smooth motions as well as maintaining the stability of the system. All of the paths designed in this article are designed to avoid mechanical damage to the actuator, and also all constraint motions of micro-positioner to be considered. They are as follows:

Path A: this path will simulate the micro-positioner movement to the desired position. This path simulates the movement of a tiny object to the desired position during a smooth path.
Path B: this path will simulate the micro-positioner movement to the desired position and stop for a moment and then return to the start point. This path simulates the gripping of a microparticle with a controllable applied force.
Path C: this path will simulate the micro-positioner movement to the desired position and stop for a moment and then return to the start point as periodic motion.

A comparison between the desired paths and tracked paths is presented in Figure 4. This figure demonstrates that the controller can successfully follow the desired paths.

The associated tracking error is illustrated in Figure 5. This figure demonstrated that the maximum error of the designed controller in tracking the input paths is less than 0.02 nm, which is less the 0.01% of the maximum desired position.

Figure 6 depicts the control effort of the system for the three mentioned paths, under the PID controller. According to these simulations, the PID controller demonstrates excellent tracking ability and control effort. Also, results in comparison of Vagia et al.[17] controller approaches indicate the effectiveness of the designed PID controller in this article not only for lower tracking error but also for less control effort.

Conclusion

In this article, the feedback linearization technique is cooperated with a PID controller to control the position of micro-actuator as well as to suppress its vibration. The micro-positioner is modeled as an Euler–Bernoulli cantilever beam. The governing equation of micro-positioner is obtained using the 1-DOF lumped-parameter model. To investigate the path tracking capability of the designed controller, three different paths from the starting position to the final point are considered. Investigating the error and control effort of the proposed controller demonstrated that the designed PID controller is effective for tracking an arbitrary path for reducing both tracking error and control effort.

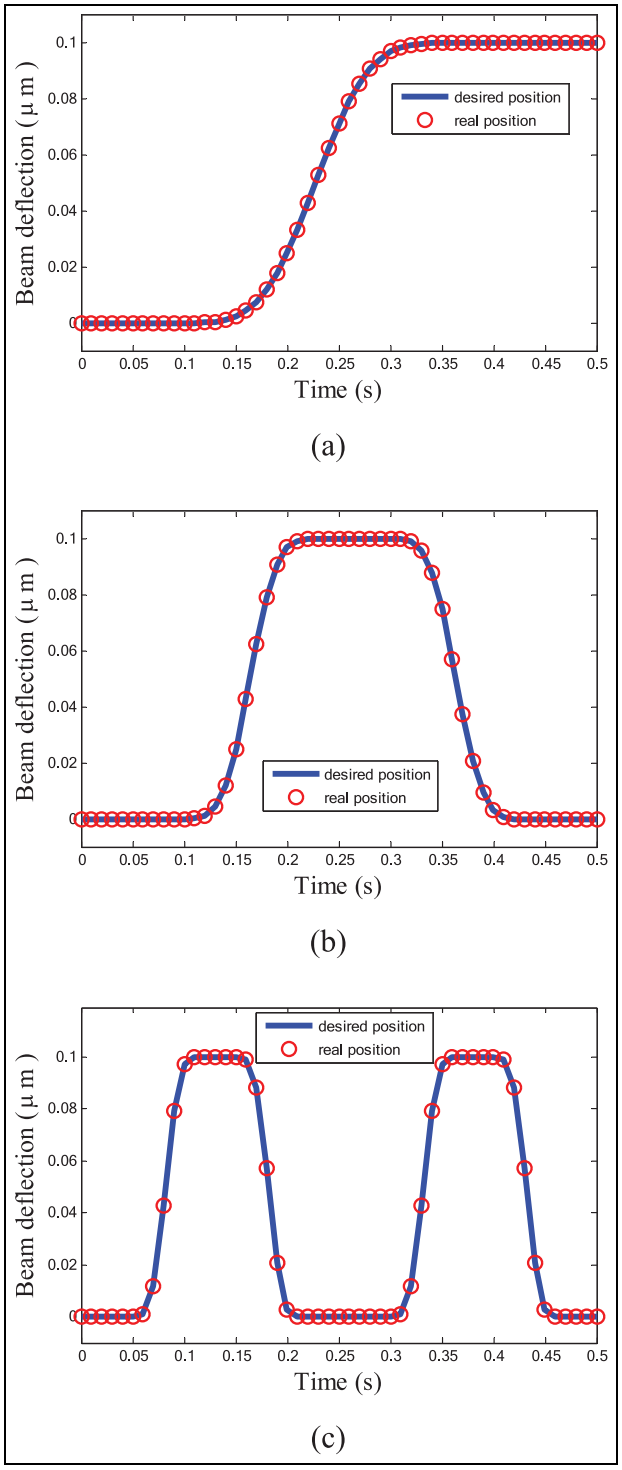

Figure 4. Controller path tracking: (a) Path A, (b) Path B, and (c) Path C.

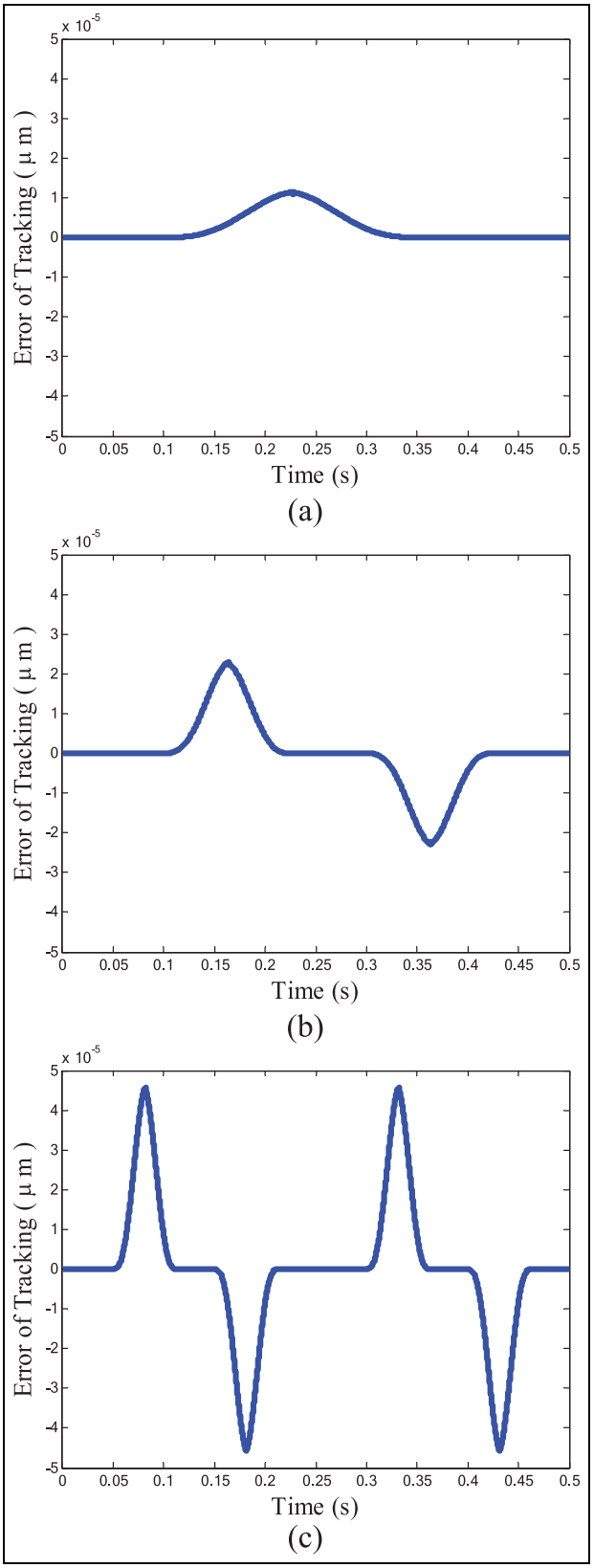

Figure 5. Tracking error of designed controller: (a) Path A, (b) Path B, and (c) Path C.

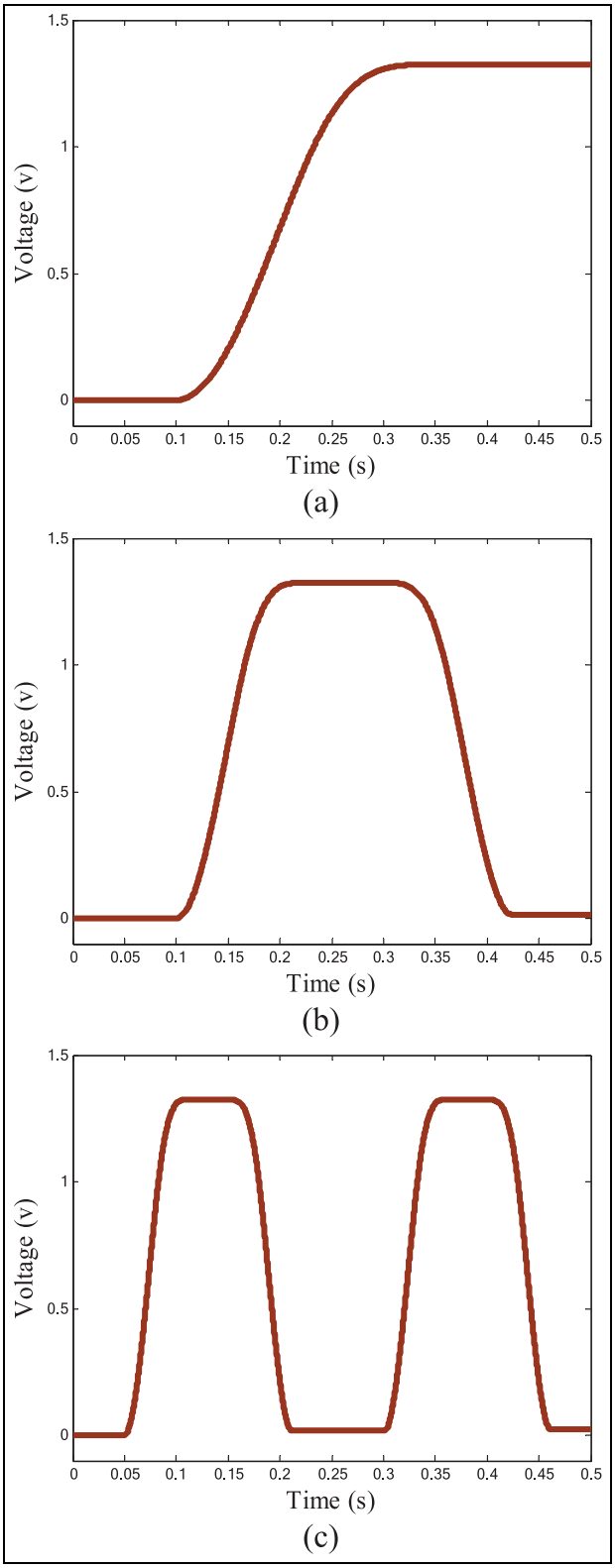

Figure 6. Control effort of the system: (a) Path A, (b) Path B, and (c) Path C.

Declaration of conflicting interests

The author(s) declared no potential conflicts of interest with respect to the research, authorship, and/or publication of this article.

Funding

The author(s) disclosed receipt of the following financial support for the research, authorship, and/or publication of this article: This work was financially supported by the Research Deputy of Education and Research, University of Torbat Heydarieh (grant no. 53).

ORCID iD

Ali Koochi https://orcid.org/0000-0003-2260-2638

References

1. Fowler AG, Laskovski AN, Hammond AC, et al. A 2-DOF electrostatically actuated MEMS nanopositioner for on-chip AFM. *J Microelectromech Syst* 2012; 21: 771–773.
2. Hubbard NB, Culpepper ML and Howell LL. Actuators for micropositioners and nanopositioners. *Appl Mech Rev* 2006; 59: 324–334.
3. Pantazi A, Lantz MA, Cherubini G, et al. A servomechanism for a micro-electro-mechanical-system-based scanning-probe data storage device. *Nanotech* 2004; 15: S612–S621.
4. Lantz MA, Rothuizen HE, Drechsler U, et al. A vibration resistant nanopositioner for mobile parallel-probe storage applications. *J Microelectromech Syst* 2007; 16: 130–139.
5. Mobki H, Rezazadeh G, Sadeghi M, et al. A comprehensive study of stability in an electro-statically actuated micro-beam. *Int J Nonl Mech* 2013; 48: 78–85.
6. Abdi J, Koochi A, Kazemi AS, et al. Modeling the effects of size dependence and dispersion forces on the pull-in instability of electrostatic cantilever NEMS using modified couple stress theory. *Smart Mater Struct* 2011; 20: 055011.
7. Koochi A and Hosseini-Toudeshky H. Coupled effect of surface energy and size effect on the static and dynamic pull-in instability of narrow nano-switches. *Int J Appl Mech* 2015; 7: 1550064.
8. Ma JB, Jiang L and Asokanthan SF. Influence of surface effects on the pull-in instability of NEMS electrostatic switches. *Nanotech* 2010; 21: 505708.
9. Zhang Y and Zhao YP. Numerical and analytical study on the pull-in instability of micro-structure under electrostatic loading. *Sensor Actuat A: Phys* 2006; 127: 366–380.
10. Zhu G, Levine J, Praly L, et al. Flatness-based control of electrostatically actuated MEMS with application to adaptive optics: a simulation study. *J Microelectromech Syst* 2006; 15: 1165–1174.
11. Maithripala DHS, Berg J and Dayawansa WP. Control of an electrostatic MEMS using static and dynamic output feedback. *J Dynam Syst Meas Contr* 2004; 127: 443–450.
12. Shirazi FA, Velni JM and Grigoriadis KM. An LPV design approach for voltage control of an electrostatic MEMS actuator. *J Microelectromech Syst* 2011; 20: 302–311.
13. Nadal-Guardia R, Dehe A, Aigner R, et al. Current drive methods to extend the range of travel of electrostatic microactuators beyond the voltage pull-in point. *J Microelectromech Syst* 2002; 11: 255–263.

14. Seeger JI and Boser BE. Charge control of parallel-plate, electrostatic actuators and the tip-in instability. *J Microelectromech Syst* 2003; 12: 656–671.
15. Tzes A, Nikolakopoulos G, Dritsas L, et al. Multi-parametric H_∞ control of a micro actuator. *IFAC P Vol* 2005; 38: 964–969.
16. Vagia M, Nikolakopoulos G and Tzes A. Intelligent robust controller design for a micro-actuator. *J Intel Robot Syst* 2006; 47: 299–315.
17. Vagia M, Nikolakopoulos G and Tzes A. Design of a robust PID-control switching scheme for an electrostatic micro-actuator. *Contr Eng Pract* 2008; 16: 1321–1328.
18. Vagia M. How to extend the travel range of a nanobeam with a robust adaptive control scheme: a dynamic surface design approach. *ISA Trans* 2013; 52: 78–87.
19. Rajaei A, Vahidi-Moghaddam A, Ayati M, et al. Integral sliding mode control for nonlinear damped model of arch microbeams. *Microsyst Tech* 2019; 25: 57–68.
20. Vagia M. A frequency independent approximation and a sliding mode control scheme for a system of a microcantilever beam. *ISA Trans* 2012; 51: 325–332.
21. Fazlyab M, Pedram MZ, Salarieh H, et al. Parameter estimation and interval type-2 fuzzy sliding mode control of a z-axis MEMS gyroscope. *ISA Trans* 2013; 52: 900–911.
22. Ghanbari A and Moghanni-Bavil-Olyaei M. Adaptive fuzzy terminal sliding-mode control of MEMS z-axis gyroscope with extended Kalman filter observer. *Syst Sci Contr Eng* 2014; 2: 183–191.
23. Hosseini-Pishrobat M and Keighobadi J. Robust vibration control and angular velocity estimation of a single-axis MEMS gyroscope using perturbation compensation. *J Intel Robot Syst* 2019; 94: 61–79.
24. Lin WH and Zhao YP. Casimir effect on the pull-in parameters of nanometer switches. *Microsyst Tech* 2005; 11: 80–85.
25. Koochi A, Hosseini-Toudeshky H, Ovesy H, et al. Modeling the influence of surface effect on instability of nanocantilever in presence of Van der Waals force. *Int J Struct Stab Dynam* 2013; 13: 1250072.
26. Lin W-H and Zhao Y-P. Pull-in instability of microswitch actuators: model review. *Int J Nonl Sci Numer Simul* 2008; 9: 175–183.